Theoretical Nitrogen NMR Chemical Shifts in Octahedral Boron Nitride Cages

Verónica Barone, Andrew Koller, and Gustavo E. Scuseria*

Department of Chemistry, Rice University, Houston, Texas 77005

Received: June 18, 2006; In Final Form: July 20, 2006

We have calculated the geometrical structure, relative stability, and nitrogen chemical shifts of five boron nitride hollow octahedral cages using density functional theory. Our results show three typical ranges for nitrogen chemical shifts corresponding to each of the nonequivalent magnetic sites of the N atoms. The principal component of the electric field gradient tensor at each ^{14}N site in boron nitride cages is predicted to be much smaller than the corresponding value in borazine, which should reflect in sharper spectral lines and much better resolution.

Introduction

After the discovery of C_{60}, higher fullerenes,[1] and carbon nanotubes,[2] other non-carbon nanostructures such as BN,[3] MoS_2, WS_2, V_2O_5, and $H_3Ti_2O_7$ nanotubes were synthesized.[4] Among the many inorganic materials with distinct structural and geometrical features, free-standing hollow nanostructures belong to an important class because of their potential applications in photonic devices, active material encapsulation, drug delivery, surface functionalization, and sensors, among others.[5]

It was theoretically predicted by computational models that octahedral cages of B_xN_x[6−8] with perfect BNBN alternation should be stable with respect to other possible structures due to the lowering of their strain energy and aromatic destabilization.[7] Furthermore, Seifert et al.[8] predicted some particular octahedral cages ($x = 12$, 16, and 28) to be energetically more favorable than others. The experimental confirmation of these theoretical results was presented by Stéphan et al.[9] when they reported the formation of boron nitride nested cages with unambiguous octahedral geometries. Many other experimental works reconfirmed the octahedral model.[10−14] The relative stability and electronic properties of different isomers of B_xN_x clusters have been studied theoretically.[15−21]

Despite these theoretical and experimental papers, the structures synthesized in the experiments are still uncertain. For instance, $B_{24}N_{24}$ clusters were synthesized in large quantities and identified by mass spectrometry,[14] and the structure containing four-membered rings, hexagons, and octagons was found theoretically to be the most stable.[22] Zope et al.[21] presented a detailed theoretical paper on the stability and Raman spectrum of $B_{36}N_{36}$ in order to help in a conclusive assignment of the proposed geometry of the cluster observed in an electron-beam irradiation experiment.[10] Experimental spectroscopic data are needed in order to be able to determine the actual structure of the cages produced in each experiment.

Nuclear magnetic resonance (NMR) has been widely utilized in chemistry, biochemistry, and solid-state chemistry for structural assignment. More recently, ^{13}C NMR chemical shifts provided evidence of the icosahedral structure of C_{60}[23] and the D_{5h} symmetry of C_{70}.[23,24] Other papers have concentrated on the ^{13}C NMR chemical shift of higher fullerenes[25−28] and, in some cases, correlated ^{13}C chemical shifts with the local strain of the fullerenes.[27] Also, ^{13}C spin−spin coupling constants in C_{70} have been calculated[29] using density functional theory (DFT) in excellent agreement with experiments.[24,30]

In contrast, little is known experimentally or theoretically about the NMR spectra of BN cages. While calculations of nitrogen chemical shifts are relatively simple, the problem is complicated experimentally. There are two naturally occurring isotopes of N, ^{14}N with natural abundance of 99.635% and nuclear spin $I = 1$ and ^{15}N with natural abundance of 0.365% and spin $I = 1/2$. Despite its rich natural abundance, ^{14}N also presents an electric quadrupole moment which broadens the NMR signal and makes accurate experimental assignments challenging. This is the reason ^{15}N is the nucleus of choice for NMR. However, the synthesis of BN cages is still in its infancy and therefore it seems very unlikely to obtain ^{15}N-enriched samples. Nonetheless, ^{14}N chemical shifts have been measured in substituted borazines by Wrackmeyer et al.[31] and Framery et al.[32]

In this work, we analyze the possibility of determining the structure of BN cages on the basis of NMR spectroscopy, which would provide another route for revealing their geometrical structure and symmetry. We report theoretical DFT calculations of nitrogen chemical shifts for five B_nN_n cages for $n = 12$, 16, 28, 36, and 48.

Computational Details

All the calculations in the present study have been performed using the development version of the *Gaussian* program.[33] We have employed the B3LYP[34]/cc-PVDZ level of theory for geometry optimizations and the B3LYP/cc-PVTZ level of theory to obtain chemical shifts using the gauge including atomic orbitals (GIAO)[35] formalism. In this work, we neglect medium effects as well as vibrational corrections. For interesting review articles about theoretical aspects of NMR chemical shifts, we refer the reader to refs 36 and 37.

Although several papers assessing density functional methods for the calculation of NMR parameters have recently appeared,[38,39] N atoms bonded to B atoms are not included in the test sets of such studies. Therefore, it is important to verify the validity of our approach by calculating N chemical shifts in boron nitride compounds with available experimental values. We have used borazine, *N*,*N*′,*N*″-trimethylborazine, *N*,*N*′-bis-

10.1021/jp063792d CCC: $33.50
Published on Web 08/24/2006

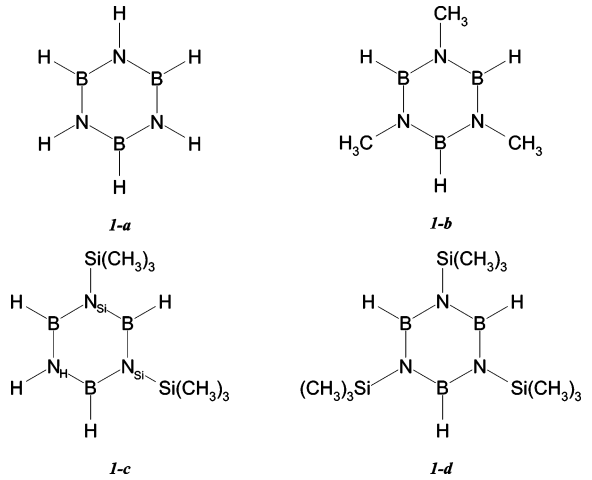

Figure 1. Schematic representation of borazine (*1-a*), *N,N′,N″*-trimethylborazine (*1-b*), *N,N′*-bis(trimethylsilyl)borazine (*1-c*), and *N,N′,N″*-tris(trimethylsilyl)borazine *(1-d)*.

TABLE 1: ^{14}N Chemical Shifts (δ) for Borazine (*1-a*), *N,N′,N″*-Trimethylborazine (*1-b*), *N,N′*-Bis(trimethylsilyl)borazine (*1-c*), and *N,N′,N″*-Tris(trimethylsilyl)borazine (*1-d*) Calculated at the B3LYP/cc-PVDZ Geometry Using GIAOS[a,b]

	δ^{14}N (ppm)					
functional/ compound	*1-a*	*1-b*	*1-c* N_H	*1-c* N_{Si}	*1-d*	MAE[c]
LSDA	−232.7	−225.2	−226.1	−208.6	−206.2	40.3
BLYP	−242.0	−233.3	−234.9	−222.2	−221.4	29.3
PBE	−233.1	−225.4	−226.2	−213.4	−210.9	38.3
KT2	−231.6	−224.7	−224.9	−211.6	−209.0	39.8
VSXC	−237.8	−226.6	−231.3	−231.3	−211.6	32.4
TPSS	−241.9	−234.8	−235.0	−225.9	−223.8	27.8
B3LYP	−272.8	−266.2	−265.6	−254.7	−252.5	2.4
B97-2	−268.6	−263.0	−261.5	−252.7	−250.5	2.3
PBE0	−271.2	−266.0	−264.2	−254.0	−251.8	2.2
experimental	−266.0	−267.3	−260.5	−254.5	−252.2	

[a] Chemical shifts refer to nitromethane at the same level of theory. [b] Experimental values from ref 31. [c] Mean Absolute Error.

(trimethylsilyl)borazine, and *N,N′,N″*-tris(trimethylsilyl)borazine[31] to perform such a comparison. In Figure 1, we present a schematic representation of these compounds. In Table 1, we present ^{14}N chemical shifts (δ) with respect to nitromethane obtained at different levels of theory. For this benchmarking purpose, we have employed nine density functionals from different families: LSDA[40] (local density approximation), BLYP,[41] PBE,[42] and KT2[43] (generalized gradient approximation, GGA), VSXC,[44] and TPSS[45] (meta-GAA), and the hybrid functionals B3LYP,[34] B97-2,[46] and PBE0.[47] From the table, we observe that δ is extremely sensitive to the functional employed to perform the GIAO calculations. The hybrid functionals B3LYP, B97-2, and PBE0 are much better choices for these borazines than the generalized gradient approximation and meta-generalized gradient approximation functionals. Mean absolute errors for the hybrids are of about 2.3 ppm. The substituent effect of H in compound *1-a* of Figure 1 is not well reproduced by any functional. This chemical shift presents the largest deviation with respect to the experiment (about 5 ppm for B3LYP). Nonetheless, we expect that these good results in borazines for hybrid functionals extrapolate to boron nitride cages.

Results

The hollow BN cages under consideration are formed solely by four- and six-membered rings. All of them have six four-membered rings corresponding to the vertexes of the octahedral structures. The number of nonequivalent nitrogen sites in each cage depends on the symmetry of the cage as well as the number of hexagons. For instance, in the smallest $B_{12}N_{12}$ cages all nitrogen atoms are magnetically equivalent, while in the biggest $B_{48}N_{48}$ cage there are three nonequivalent N sites. In Figure 2(I−V), we present the scheme of each of the BN cages studied here. Boron atoms are shown in gray, while the different magnetic sites for nitrogen atoms are shown in red, blue, and yellow whether they correspond to a nitrogen belonging to a four-membered ring (N_A, red), a nitrogen belonging to a hexagon and surrounded by three hexagons and a four-membered ring (N_B, blue), and a nitrogen atom belonging to a hexagon that is surrounded only by six-membered rings (N_C, yellow).

In Table 2, we summarize our results for boron−nitrogen bond lengths (as defined in Figure 2), relative energies, HOMO-LUMO gaps, π-orbital axis vector (POAV) angle,[48] average radii, and nitrogen chemical shifts for each cage. The POAV vector is defined as the one that makes equal angles simultaneously with the three σ bonds. The POAV pyramidalization angle is $\pi/2$ minus this common angle and can be related to the local strain of a given cage.[27,49]

As reported previously,[7] we observe that the binding energies increase with the cage size. As expected, the local strain of the structures measured by the POAV angle decreases as the size of the cages increases, with the POAV angle of N_B ranging from 16.9 to 11.7 degrees and the POAV angle of N_C ranging from 10.9 to 8.6 degrees. The only exception corresponds to the nitrogen atoms belonging to the four-membered rings, N_A, in which the POAV angle for the largest cage is 26.1 degrees while in the smallest it is 26.4 degrees. The local strain at these sites is quantified by the large POAV angles of the N_A atoms. For the nitrogen atoms N_A and N_C, we also observe a slight decrease in the B−N bond lengths (a_1, a_2, and a_3, and c_1, c_2, and c_3, respectively) as the size of the cages increases.

Regarding the NMR spectra of BN cages, there are three signature ranges for nitrogen chemical shifts (with respect to nitromethane) in these compounds. For N_A, the chemical shift for different cages varies from −245.2 to −259.0 ppm. For N_B, the absolute value of δN is maximum, and the chemical shift ranges between −276.9 and −287.0 ppm. Finally, the intermediate range corresponds to the N_C atom in yellow for which the planar geometry surrounding it resembles more closely borazine and substituted borazines and the chemical shift ranges between −253.6 and −269.0 ppm. Chemical shifts for a given type of nitrogen do not present any apparent relation with geometrical parameters. However, it is difficult to conclusively determine this kind of trend here due to the relatively small number of cages under study.

Another interesting feature in a NMR experiment is the relative intensity of each of the peaks for a given cage. In the small $B_{12}N_{12}$ cage, we should observe a single line corresponding to N_A. The next cage in size, $B_{16}N_{16}$, should present two lines with relative intensities 3:1, while the remaining cages present 3 lines each with intensities 3:3:1 ($B_{28}N_{28}$), 1:1:1 ($B_{36}N_{36}$), and 1:1:2 ($B_{48}N_{48}$).

The accuracy to which the position of a ^{14}N line may be determined in the experiment is limited by its broad nature. Typically, the ^{15}N spectra display narrow lines with widths usually smaller than 10 Hz. In contrast, ^{14}N lines present widths greater than 100 Hz. This difference enables ^{15}N line positions

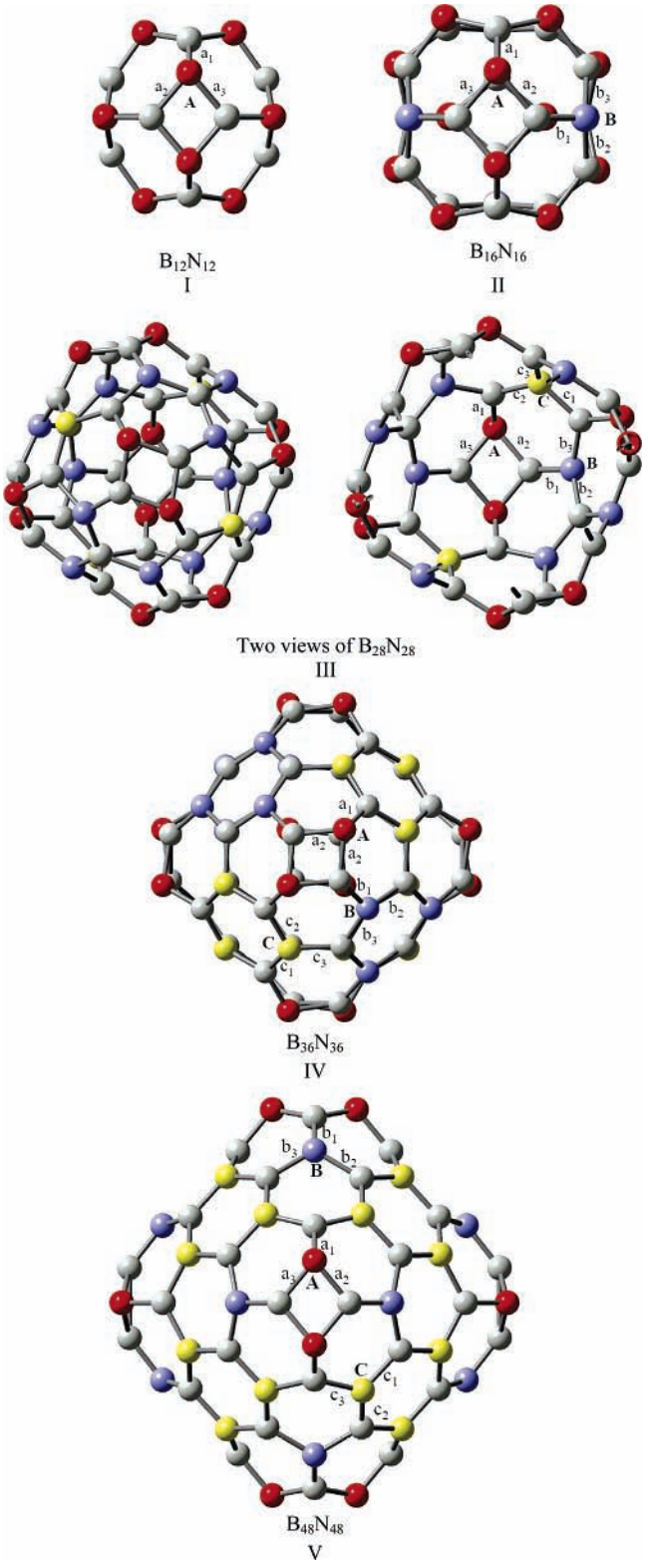

Figure 2. The boron nitride cages.

to be determined to a greater accuracy than is possible for those of ^{14}N, permitting the study of small chemical shift differences and also the measurement of spin−spin coupling constants.

In general, the spin relaxation mechanism is dominated by the quadrupolar relaxation. In this situation, the width of the spectral lines of ^{14}N is proportional to the square of the principal component of the electric field gradient tensor (eq_{zz}) at the nucleus position.[50] Therefore, the smaller eq_{zz} is, the narrower

TABLE 2: Symmetry Groups, Relative Energies, HOMO-LUMO Gaps, and Geometrical Parameters (bond lengths as indicated in Figure 2 and radii in Å, and POAV angles in degrees) for the Five Boron Nitride Cages Obtained at the B3LYP/cc-PVDZ Level of Theory[a]

cage	$B_{12}N_{12}$	$B_{16}N_{16}$	$B_{28}N_{28}$	$B_{36}N_{36}$	$B_{48}N_{48}$
point group	T_h	T_d	T	T_d	T_h
E/atom (kcal/mol)[b]	10.7	7.2	3.1	1.8	0.00
gap (eV)	6.7	6.3	6.7	6.7	6.6
a_1	1.442	1.461	1.437	1.438	1.435
a_2	1.489	1.476	1.470	1.466	1.468
a_3	1.489	1.476	1.470	1.466	1.468
POAV-A	26.4	24.6	25.6	26.2	26.1
number of N_A	12	12	12	12	12
δN_A (ppm)	−259.0	−245.7	−248.7	−248.7	−245.2
b_1		1.457	1.483	1.428	1.424
b_2		1.457	1.429	1.468	1.471
b_3		1.457	1.476	1.468	1.471
POAV-B		16.9	12.3	10.9	11.7
number of N_B		4	12	12	12
δN_B (ppm)		−283.6	−276.9	−283.8	−287.0
c_1			1.478	1.483	1.471
c_2			1.478	1.467	1.447
c_3			1.478	1.467	1.467
POAV-C			10.9	10.3	8.6
number of N_C			4	12	24
δN_C (ppm)			−253.6	−264.3	−269.0
R_{av}[c]	2.302	2.626	3.418	3.934	4.623

[a] Nitrogen chemical shifts with respect to nitromethane obtained using GIAO at the B3LYP/ cc-PVTZ level of theory. [b] Energies relative to $B_{48}N_{48}$. [c] Average atomic distance to the geometric center.

TABLE 3: Absolute Value of the Principal Component of the Electric Field Gradient Tensor (eq_{zz}) in Atomic Units for Borazine, *N,N′,N″*-Trimethylborazine, and the Boron Nitride Cages at Each of the Nonequivalent ^{14}N Sites at the B3LYP/ cc-PVTZ Level of Theory

compound	^{14}N site	eq_{zz} (au)
1-a		0.344
1-b		0.472
1-c	N_H	0.349
1-c	N_{Si}	0.039
1-d		0.046
$B_{12}N_{12}$	A	0.141
$B_{16}N_{16}$	A	0.133
	B	0.170
$B_{28}N_{28}$	A	0.055
	B	0.218
	C	0.153
$B_{36}N_{36}$	A	0.041
	B	0.231
	C	0.186
$B_{48}N_{48}$	A	0.042
	B	0.236
	C	0.112

the spectral lines become, and it is possible, in some cases, to better resolve the NMR spectrum. For instance, Wrackmeyer et al.[31] experimentally found that for some particular substituents in borazines, line widths of ^{14}N signals can be as narrow as 5.0 Hz at room temperature. These authors also calculated eq_{zz} for the substituted borazines and found that in those with the sharper spectral lines, eq_{zz} at the N site was significantly smaller. Therefore, it is interesting to compare the calculated eq_{zz} values for borazines and boron nitride cages to evaluate the feasibility of experimental assignments of N chemical shifts at natural abundance. In Table 3, we present our results for eq_{zz} at the position of each ^{14}N atom, obtained at the same level of theory as nitrogen chemical shifts. We find that eq_{zz} is significantly smaller in the cages than in the compounds depicted in Figure 1, compounds *1-a* and *1-b*. As shown experimentally, this effect

should reflect in sharper NMR peaks.[31] This is particularly apparent in N_A of the three largest cages under study for which the spectral line should be tenths of times narrower than the corresponding line in borazine. We could also speculate that this enhanced sensitivity could help to measure the $^1J(^{14}N,^{11}B)$ coupling constant in these cages. As studied by Wrackmeyer et al.,[31] the experimental value of $^1J(^{14}N,^{11}B)$ for compound *1-d* is 23.0 ± 0.5 Hz. Our calculated $^1J(^{14}N,^{11}B)$ in this compound at the B3LYP/cc-PVTZ level is 22.6 Hz. Due to the excellent agreement between the experiment and theory for *N*,*N*′,*N*″-tris-(trimethylsilyl)borazine, we can also attempt to predict $^1J(^{14}N,^{11}B)$ in the boron nitride cages. As spin−spin couplings are computationally demanding, we report here only one-bond couplings for the two smallest cages, $B_{12}N_{12}$ and $B_{16}N_{16}$. In the cage $B_{12}N_{12}$, only two one-bond couplings are present: $^1J(^{14}N_a,^{11}B_1) = 19.2$ Hz and $^1J(^{14}N_a,^{11}B_{2,3}) = 8.1$ Hz. Two magnetically nonequivalent N sites are present in the cage $B_{16}N_{16}$ giving rise to three different one-bond couplings: $^1J(^{14}N_a,^{11}B_1) = 13.5$ Hz and $^1J(^{14}N_a,^{11}B_{2,3}) = 6.7$ Hz for N_a and just one coupling for N_b: $^1J(^{14}N_b,^{11}B_{1,2,3}) = 14.2$ Hz. The values of $^1J(^{14}N,^{11}B)$ in the BN cages seem related to the N−B bond length (see Table 1).

Conclusions

We have calculated the geometrical structure, relative stability, and nitrogen chemical shifts of five boron nitride hollow octahedral cages using density functional theory. Our results show three typical ranges for δN corresponding to each of the nonequivalent magnetic sites of the N atoms. Although in general ^{14}N NMR is far less sensitive than ^{15}N, we find that the principal component of the electric field gradient tensor at each ^{14}N site in BN cages is much smaller than the corresponding values in borazine, which should reflect in narrower spectral lines and better resolution. This effect is especially noticeable in the N atom belonging to the four-membered ring for which our calculations predict lines as sharp as in a ^{15}N isotope. Spectral widths may be further reduced by performing the experiment at low temperature. Therefore, if the sample is pure enough, ^{14}N chemical shifts in BN cages should be resolved.

Our work not only sheds light on the values of nitrogen chemical shifts in BN cages for which no NMR parameter was ever reported, but also predicts sharp lines in the NMR spectrum of these compounds at natural abundance. Experimental spectroscopic data in BN cages will be necessary in order to verify our predictions and conclusively determine the structures produced in experiments.

Acknowledgment. This work was supported by NSF Award Number CHE-0457030 and the Welch Foundation. Calculations were performed in part on the Rice Terascale Cluster funded by NSF under Grant EIA-0216467, Intel, and HP. V.B. thanks Dr. J. E. Peralta for kindly providing the coordinates of the cages and Prof. R. H. Contreras, Prof. B. Wrackmeyer, and Dr. L. B. Alemany for fruitful comments.

References and Notes

(1) Kroto, H. W.; Health, J. R.; O'Brien, S. C.; Curl, R. F.; Smalley, R. E. *Nature* **1985**, *318*, 162.

(2) Iijima, S. *Nature* **1991**, *354*, 56.

(3) Chopra, N. G.; Luyken, R. J.; Cherrey, K.; Crespi, V. H.; Cohen, M. L.; Louie, S. G.; Zettl, A. *Science* **1995**, *269*, 966.

(4) Tenne, R. *Angew. Chem., Int. Ed.* **2003**, *42*, 5124.

(5) Zeng, H. C. *J. Mater. Chem.* **2006**, *16*, 649.

(6) Jensen, F.; Toflund, H. *Chem. Phys. Lett.* **1993**, *201*, 89.

(7) Zhu, H. Y.; Schmaltz, T. G.; Klein, D. J. *Int. J. Quantum Chem.* **1997**, *63*, 393.

(8) Seifert, G.; Fowler, R. W.; Mitchell, D.; Porezag, D.; Frauenheim, T. *Chem. Phys. Lett.* **1997**, *268*, 352.

(9) Stéphan, O.; Bando, Y.; Loiseau, A.; Willaime, F.; Shramchenko, N.; Tamiya, T.; Sato, T. *Appl. Phys. A: Mater. Sci. Process.* **1998**, *67*, 107.

(10) Golberg, D.; Bando, Y.; Stéphan, O.; Kurashima, K. *Appl. Phys. Lett.* **1998**, *73*, 2441.

(11) Oku, T.; Hirano, T.; Kuno, M.; Kusunose, T.; Niihara, K.; Suganuma, K. *Mater. Sci. Eng. B* **2000**, *74*, 206.

(12) Bengu, E.; Marks, L. D. *Phys. Rev. Lett.* **2001**, *86*, 2385.

(13) Pokropivny, V. V.; Skorokhod, V. V.; Oleinik, G. S.; Kurdyumov, A. V.; Bartnitskaya, T. S.; Pokropivny, A. V.; Sisonyuk, A. G.; Sheichenko, D. M. *J. Solid State Chem.* **2000**, *154*, 214.

(14) Oku, T.; Nishiwaki, A.; Narita, I.; Gonda, M. *Chem. Phys. Lett.* **2003**, *380*, 620.

(15) Zhu, H.-Y.; Schmalz, T. G.; Klein, D. J. *Int. J. Quantum Chem.* **1997**, *63*, 393.

(16) Wu, H.-S.; Xu, X.-H.; Strout, D. L.; Jiao, H. *J. Mol. Model* **2005**, *12*, 1.

(17) Strout, D. L. *Chem. Phys. Lett.* **2004**, *383*, 95.

(18) Strout, D. L. *J. Phys. Chem. A* **2001**, *105*, 261.

(19) Zope, R. R.; Dunlap, B. I. *Chem. Phys. Lett.* **2004**, *386*, 403.

(20) Zope, R. R.; Baruah, T.; Pederson, M. R.; Dunlap, B. I. *Chem. Phys. Lett.* **2004**, *393*, 300.

(21) Zope, R. R.; Baruah, T.; Pederson, M. R.; Dunlap, B. I. *Phys. Rev. A* **2005**, *71*, 025201.

(22) Wu, H.-S.; Jiao, H. *Chem. Phys. Lett.* **2004**, *386*, 369.

(23) Taylor, R.; Hare, J. P.; Abdul-Sada, A. K.; Kroto, H. W. *J. Chem. Soc. Chem. Commun.* **1990**, *20*, 1423.

(24) Johnson, R. D.; Meijer, G.; Salem, J. R.; Bethune, D. S. *J. Am. Chem. Soc.* **1991**, *113*, 3619.

(25) Taylor, R.; Langley, G. J.; Avent, A. G.; Dennis, T. J. S.; Kroto, H. W.; Walton, D. R. M. *J. Chem. Soc., Perkin Trans.* **1993**, *2*, 1029.

(26) Kikuchi, K.; Nakahara, N.; Wakabayashi, T.; Suzuki, S.; Shiromaru, H.; Miyake, Y.; Saito, K.; Ikemoto, L.; Kainosho, M.; Achiba, Y. *Nature* **1992**, *357*, 142.

(27) Heine, T.; Seifert, G.; Fowler, P. W.; Zerbetto, F. *J. Phys. Chem. A* **1999**, *103*, 8738.

(28) Sun, G.; Kertesz, M. *J. Phys. Chem. A* **2000**, *104*, 7398.

(29) Peralta, J. E.; Barone, V.; Scuseria, G. E.; Contreras, R. H. *J. Am. Chem. Soc.* **2004**, *126*, 7428.

(30) Anklin, C.; Alemany, L. B. *Magn. Reson. Chem.* **2006**, *44*, 230.

(31) Wrackmeyer, B.; Schwarze, B.; Durran, D. M.; Webb, G. A. *Magn. Reson. Chem.* **1995**, *33*, 557.

(32) Framery, E.; Vaultier, M. *Heteroatom Chem.* **2000**, *11*, 218.

(33) Frisch, M. J., et al. *Gaussian*, Development version, Revision C-1; Gaussian, Inc.: Pittsburgh, PA, 2003.

(34) Becke, A. D. *J. Chem. Phys.* **1993**, *98*, 5648.

(35) Dodds, J. L.; McWeeny, R.; Sadlej, A. J. *Mol. Phys.* **1980**, *41*, 1419.

(36) Helgaker, T.; Jaszunski, M.; Ruud, K. *Chem. Rev.* **1999**, *99*, 293.

(37) de Dios, A. C.; Jameson, C. J. *Ann. Rep. NMR Spectrosc.* **1994**, *29*, 1.

(38) Allen, M. J.; Keal, T. W.; Tozer, D. J. *Chem. Phys. Lett.* **2003**, *380*, 70.

(39) Maximoff, S. N.; Scuseria, G. E. *Chem. Phys. Lett.* **2004**, *390*, 408.

(40) Vosko, S. H.; Wilk, L.; Nusair, M. *Can. J. Phys.* **1980**, *58*, 1200.

(41) Lee, C.; Yang, W.; Parr, R. G. *Phys. Rev. B* **1988**, *37*, 785.

(42) Perdew, J. P.; Burke, K.; Ernzerhof, M. *Phys. Rev. Lett.* **1996**, *77*, 3865.

(43) Keal, T. W.; Tozer, D. J. *J. Chem. Phys.* **2003**, *119*, 3015.

(44) Van Voorhis, T.; Scuseria, G. E. *J. Chem. Phys.* **1998**, *109*, 400.

(45) Tao, J.; Perdew, J. P.; Staroverov, V. N.; Scuseria, G. E. *Phys. Rev. Lett.* **2003**, *91*, 146401.

(46) Wilson, P. J.; Bradley, T. J.; Tozer, D. J. *J. Chem. Phys.* **2001**, *115*, 9233.

(47) Perdew, J. P.; Burke, K.; Ernzerhof, M. *Phys. Rev. Lett.* **1996**, *77*, 3865.

(48) Haddon, R. C.; Scott, L. T. *Pure Appl. Chem.* **1986**, *58*, 137.

(49) Haddon, R. C.; Scuseria, G. E.; Smalley, R. E. *Chem. Phys. Lett.* **1997**, *272*, 38.

(50) Kidd, R. G.; Goodfellow, R. J. In *NMR and the Periodic Table*; Harris, R. K., Mann, B. E., Eds.; Academic: New York, 1978; p 195.